Phospho-regulation of kinesin-5 during anaphase spindle elongation

Rachel Avunie-Masala[1,*], Natalia Movshovich[2,*], Yael Nissenkorn[1,3], Adina Gerson-Gurwitz[2], Vladimir Fridman[1], Mardo Kõivomägi[4], Mart Loog[4], M. Andrew Hoyt[5], Arieh Zaritsky[3] and Larisa Gheber[1,2,‡]

[1]Department of Clinical Biochemistry, [2]Department of Chemistry, [3]Department of Life Sciences, Ben-Gurion University of the Negev, PO Box 653, Beer-Sheva, 84105, Israel
[4]Institute of Technology, University of Tartu, Tartu 50411, Estonia
[5]Department of Biology, The Johns Hopkins University, Baltimore, MD 21218, USA

*These authors contributed equally to this work
‡Author for correspondence (lgheber@bgu.ac.il)

Accepted 11 November 2010
Journal of Cell Science 124, 873-878

doi:10.1242/jcs.077396

Summary

The kinesin-5 *Saccharomyces cerevisiae* homologue Cin8 is shown here to be differentially phosphorylated during late anaphase at Cdk1-specific sites located in its motor domain. Wild-type Cin8 binds to the early-anaphase spindles and detaches from the spindles at late anaphase, whereas the phosphorylation-deficient Cin8-3A mutant protein remains attached to a larger region of the spindle and spindle poles for prolonged periods. This localization of Cin8-3A causes faster spindle elongation and longer anaphase spindles, which have aberrant morphology. By contrast, the phospho-mimic Cin8-3D mutant exhibits reduced binding to the spindles. In the absence of the kinesin-5 homologue Kip1, cells expressing Cin8-3D exhibit spindle assembly defects and are not viable at 37°C as a result of spindle collapse. We propose that dephosphorylation of Cin8 promotes its binding to the spindle microtubules before the onset of anaphase. In mid to late anaphase, phosphorylation of Cin8 causes its detachment from the spindles, which reduces the spindle elongation rate and aids in maintaining spindle morphology.

Key words: Cdk1, Cin8, Kinesin-5, Microtubules, Mitosis

Introduction

Evolutionary conserved homotetrameric kinesin-5 motor proteins have major roles in mitotic spindle morphogenesis (Blangy et al., 1995; Goshima and Vale, 2005; Hagan and Yanagida, 1992; Heck et al., 1993; Hoyt et al., 1992). These motors crosslink and slide antiparallel microtubules (Gheber et al., 1999; Kapitein et al., 2005) originating from opposite spindle poles, thereby performing their mitotic functions (Kashina et al., 1997). In addition to their well-established roles in spindle assembly (Hoyt et al., 1992), kinesin-5 motor proteins also have a role in anaphase B spindle elongation in the budding yeast *Saccharomyces cerevisiae* (Gerson-Gurwitz et al., 2009; Movshovich et al., 2008; Saunders et al., 1995; Straight et al., 1998) and other organisms (Sharp et al., 1999; Touitou et al., 2001). Although kinesin-5 motor proteins perform essential functions at several stages of spindle dynamics, and their levels are regulated in a cell-cycle-dependent manner (Gordon and Roof, 2001; Hildebrandt and Hoyt, 2001; Spellman et al., 1998), regulation of their function is not well understood. Previous reports have indicated that kinesin-5 motors are phosphorylated by mitotic kinases (Blangy et al., 1995; Chee and Haase, 2010; Garcia et al., 2009; Giet et al., 1999; Sawin and Mitchison, 1995; Sharp et al., 1999), but the mechanism by which phosphorylation regulates kinesin-5 functions is not fully understood. Here we examine the role of phosphorylation in controlling the intracellular function of the *S. cerevisiae* kinesin-5 homologue Cin8.

Results and Discussion

Cin8 is phosphorylated during anaphase in its motor domain by Cdk1

To examine the phosphorylation of Cin8 as a function of cell cycle progression, we used cells expressing Myc-tagged Cin8 that were arrested at different stages of the cell cycle. Fractionation of the cell extracts by SDS-PAGE followed by western blot analysis demonstrated that in cells arrested at late anaphase by any one of several temperature-sensitive mutations [*cdc15-2*, *cdc14-1* (Jaspersen et al., 1998) and *cdc5-7* (Park et al., 2003)], Cin8 exhibits a slow-migrating form (Fig. 1A), indicative of protein phosphorylation. This band-shift was observed for Cin8 produced either from a CEN (centromere) or 2 μm plasmid tagged with the Myc epitope either at its N- or C- terminus (Fig. 1) and for Cin8–BCP (Gheber et al., 1999) (data not shown). The slow-migrating band of Cin8 was not present in cells arrested in S-phase or in metaphase (Fig. 1B), and was abolished by treatment of the cell extracts with phosphatase (Fig. 1C). These results indicate that Cin8 is differentially phosphorylated during anaphase.

The amino acid sequence of Cin8 contains five putative phosphorylation sites for the conserved cyclin-dependent kinase 1 Cdk1 (Cdc28 in *S. cerevisiae*) ([S/T]-Px-[R/K] or [S/T]-P-[R/K]) (Langan et al., 1989; Shenoy et al., 1989). Three sites are located in the motor domain and two are in the stalk and tail. Mutation of all five amino acids to alanine (Cin8-5A) or of the three located in the motor domain (Cin8-3A) but not of the two in the stalk and tail

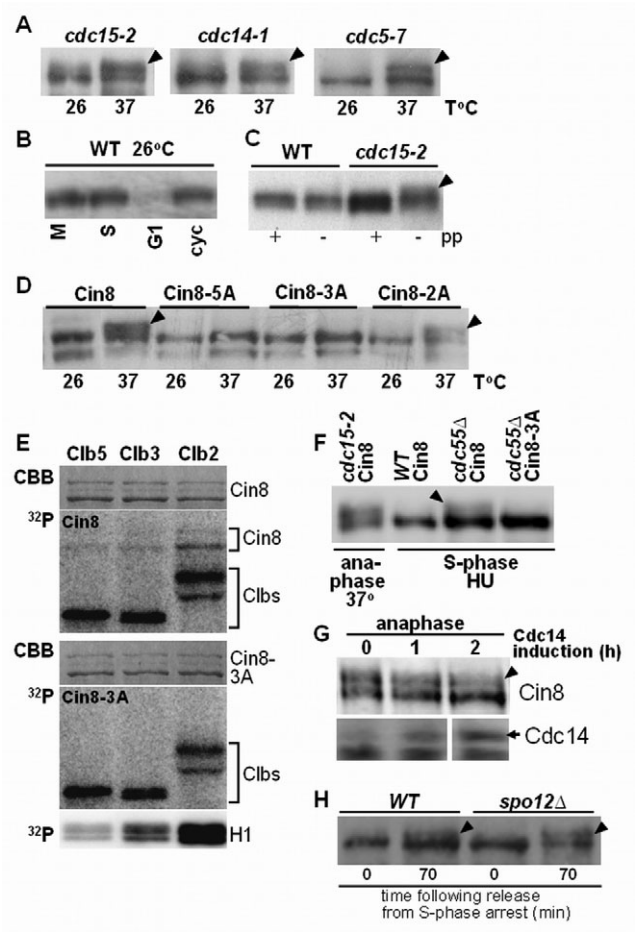

Fig. 1. Cin8 is differentially phosphorylated during anaphase. Band-retardation assay in whole extracts of cells producing 6Myc–Cin8. Extracts were fractionated on SDS-PAGE and examined by Western blot. Arrowheads indicate the slow-migrating band of Cin8. (**A**) Cells expressing *cdc15-2*, *cdc14-1* or *cdc5-7* and containing 6Myc–Cin8 were grown at 26°C (permissive) and 37°C (restrictive). (**B**) Wild-type cells were either cycling or arrested at metaphase (by nocodazole), S-phase (by hydroxyurea) and G1 (by α-factor). (**C**) WT cells or *cdc15-2* cells were grown at 37°C for 4 hours. The extracts were either treated with CIP phosphatase (pp) (+) or not (–). (**D**) *cdc15-2* cells expressing either WT Cin8, Cin8-5A (S277, T285, S493, S736, S1010), Cin8-3A (S277, T285, S493) or Cin8-2A (S736, S1010) (indicated on top) were grown at 26°C or 37°C (indicated at the bottom). (**E**) In vitro phosphorylation of bacterially expressed Cin8-590 by Cdk1 using equal concentrations of the Cdk1 complexes with cyclin Clb2, Clb3 or Clb5 (indicated on top). Coomassie Brilliant Blue (CBB) staining and ^{32}P autoradiograms of SDS-PAGE fractionation of phosphorylation reaction mixtures are shown (indicated on the left). Proteins corresponding to the various bands are indicated on the right, based on their predicted size. The relative specificity pattern obtained using equal concentrations of the kinase complexes with a reference substrate Histone H1 is shown in the bottom panel (H1). (**F**) Effect of CDC55 deletion on band-retardation assay of Cin8. Genotypes of cells and variants of Cin8–13Myc are indicated at the top; the various modes of arrest are indicated at the bottom. (**G**) Effect of Cdc14 overexpression on the slow-migrating band of Cin8–13Myc. 3HA–Cdc14 was produced from a galactose-inducible promoter. Cells were arrested either in S-phase or at late anaphase (indicated on top). In anaphase-arrested cells, Cdc14 was induced by addition of galactose for the times indicated above. The western blots of Cin8–13Myc (top) and 3HA–Cdc14 (bottom) are shown. (**H**) 6Myc–Cin8 was expressed in WT or *spo12Δ* cells (indicated on top). Cells were arrested in S-phase and released to fresh medium for 70 minutes (bottom).

(Cin8-2A), almost completely abolished the slow-migrating band of Cin8 at the end of anaphase (Fig. 1D). To examine whether Cin8 is phosphorylated by Cdk1, we performed an in vitro phosphorylation assay using a bacterially expressed truncated form of Cin8, which contains its catalytic motor domain (Cin8-590) (Hildebrandt et al., 2006). Cin8-590 was indeed phosphorylated by Cdk1, and the mitotic complex Clb2–Cdk1 showed higher specificity relative to the earlier complexes Clb3–Cdk1 and Clb5–Cdk1 (Fig. 1E). Moreover, alanine replacement of the three Cdk1-specific sites that abolish the slow-migrating band of Cin8 during anaphase (Fig. 1D) completely eliminated the phosphorylation of Cin8-3A-590 by the Clb2–Cdk1 in vitro (Fig. 1E). Consistent with these findings, it has been recently reported that Cin8 is a substrate of Clb2–Cdk1 both in vivo and in vitro (Chee and Haase, 2010). However, this recent report (Chee and Haase, 2010) does not demonstrate specifically that sites in the Cin8 motor domain are targets for Cdk1 phosphorylation. Our results indicate that during anaphase, Cin8 is phosphorylated by Clb2–Cdk1 at site(s) located within its motor domain. Moreover, in agreement with previous reports that a low Clb2–Cdk1 activity is maintained throughout anaphase (Queralt et al., 2006), our data suggest that this activity is sufficient for accumulation of the phosphorylated form of Cin8 at the end of anaphase. Alternatively, during anaphase, the same sites might be phosphorylated by an additional kinase.

Two of the three sites that abolish the Cin8 phosphorylation, S277 and T285, are located within the uniquely large loop 8 (aa 255–353) of Cin8 motor domain (Hoyt et al., 1992). The third, S493 is only 13 residues away from loop 12 and α-helix 5 in the kinesin motor domain, which are important for the interaction with microtubules (Kull et al., 1996; Sablin et al., 1996; Woehlke et al., 1997). Interestingly, S493 itself is conserved among the kinesin family members and, as in Cin8, is part of a consensus sequence for phosphorylation by Cdk1 also in the second *S. cerevisiae* kinesin-5 homologue Kip1.

Because Cdk1 is activated before anaphase (Grandin and Reed, 1993), the finding that phosphorylated Cin8 is accumulated only during anaphase (Fig. 1A,B) suggests that prior to anaphase, it is dephosphorylated by one or more phosphatases. Therefore, we examined whether the separase-dependent Ser/Thr-specific PP2A^{Cdc55} phosphatase, which dephosphorylates Cdk1 sites before anaphase onset (Queralt et al., 2006), affects the phosphorylation of Cin8. Indeed, a reproducible slow-migrating band of Cin8 was observed for *cdc55Δ* but not for WT cells arrested in S-phase with short spindles (Fig. 1F). This band was abolished when the phosphorylation-deficient mutant Cin8-3A was expressed in *cdc55Δ* cells (Fig. 1F). These results indicate that the PP2A^{Cdc55} phosphatase is involved, at least in part, in Cin8 dephosphorylation before anaphase onset. A similar regulation mechanism was previously demonstrated for inhibition of Cdk1-dependent Net1 phosphorylation before anaphase by the PP2A^{Cdc55} phosphatase (Queralt et al., 2006). Our data therefore suggest that inactivation of separase-dependent PP2A^{Cdc55} promotes phosphorylation of a number of Cdk1 targets, including Cin8, whose phosphorylation is required for anaphase progression.

To examine the possibility that the conserved Cdc14 phosphatase (Stegmeier et al., 2002) dephosphorylates Cin8 during anaphase,

the band-retardation assay was performed in cells synchronized in late anaphase by *cdc15-2* and then Cdc14 was overexpressed from a galactose-inducible promoter, while holding the late-anaphase arrest. Overexpression of Cdc14 reduced the appearance of the slow-migrating band of Cin8 in a time-dependent manner (Fig. 1G). Quantitative analysis indicates that without Cdc14 overexpression, the ratio of intensities between the slow-migrating (phosphorylation) and the low bands of Cin8 is ~1, whereas after overexpression of Cdc14 for 2 hours, this ratio drops to ~0.5.

To further explore the involvement of Cdc14 in Cin8 dephosphorylation, we examined Cin8 phosphorylation during anaphase progression in WT cells versus cells deleted for *SPO12*, a member of the early-anaphase Cdc14 activation pathway (Stegmeier et al., 2002). Seventy minutes after release from S-phase arrest, when ~60% of cells are in anaphase (not shown), a reproducible slow-migrating band appeared in both *WT* and *spo12Δ* cells (Fig. 1H). Quantitative analysis showed that in the absence of Spo12, the ratio between the slow-migrating and the low bands of Cin8 increased by 40% (Fig. 1H), indicating the deletion of *SPO12* enhances Cin8 phosphorylation. Taken together, these results show that Cdc14 is involved in Cin8 dephosphorylation during anaphase.

Cdk1 phosphorylation of Cin8 affects its localization to the mitotic spindle

Monitoring of the localization of Cin8–3GFP to the anaphase spindles in unsynchronized *WT* cells revealed that in early-mid anaphase, when spindles are shorter than 4.5–5 μm, WT Cin8 binds to a large portion of the spindle, as well as near the spindle poles (Fig. 2Aa,Ba). As spindles elongate, Cin8 was concentrated at a decreasing portion of the middle region. At late anaphase, when spindles are longer than ~8 μm, Cin8 was barely detectable at the middle spindle and was diffusively localized near the spindle poles (Fig. 2Aa). Consistent with the localization pattern in cells arrested in late anaphase by the *cdc15-2*, *cdc14-1* and *cdc5-7* mutations, when significant phosphorylation of Cin8 is detectable (Fig. 1A), Cin8 localized diffusively near the spindle poles and was not focused at the midzone (supplementary material Fig. S1).

The Cin8-2A mutant, which does not affect Cin8 phosphorylation during anaphase (Fig. 1D), exhibited similar spindle localization to that of WT Cin8 (Fig. 2Ab). Compared with WT Cin8 and Cin8-2A, the phosphorylation-deficient Cin8-3A mutant (Fig. 1D) remained localized near the spindle poles, occupied a larger portion of the middle spindle during mid-late anaphase and remained localized to this region for a longer period of time (Fig. 2Ac,Bb). Similarly to the Cin8-3A mutant, in cells that lack the Cdk1 cyclin Clb2 (*clb2Δ*), which is involved in Cin8 phosphorylation (Fig. 1E), *WT* Cin8 occupied a large portion of the anaphase spindles (supplementary material Fig. S2B). By contrast, the phospho-mimic Cin8-3D, where Cdk1 sites in the motor domain are replaced by aspartic acid, failed to bind to the spindle and exhibited diffusive localization at early anaphase (Fig. 2Ad). Also, in *cdc55Δ* cells, where Cin8 phosphorylation is increased (Fig. 1F), partial diffusive localization of Cin8 in early anaphase was observed (supplementary material Fig. S2C). Thus, taken together, our results indicate that Cin8 dephosphorylation at early anaphase is required for its attachment to the spindle, whereas phosphorylation of Cin8 leads to its detachment from the spindle at late anaphase.

Next, viability of *cin8Δ kip1Δ* cells was examined in which *CIN8* shuffle plasmid (Gheber et al., 1999) was replaced by a centromeric plasmid expressing *CIN8*, *cin8-3A* or *cin8-3D*. Cin8 and Cin8-3A cells remained viable at all examined temperatures, but cells

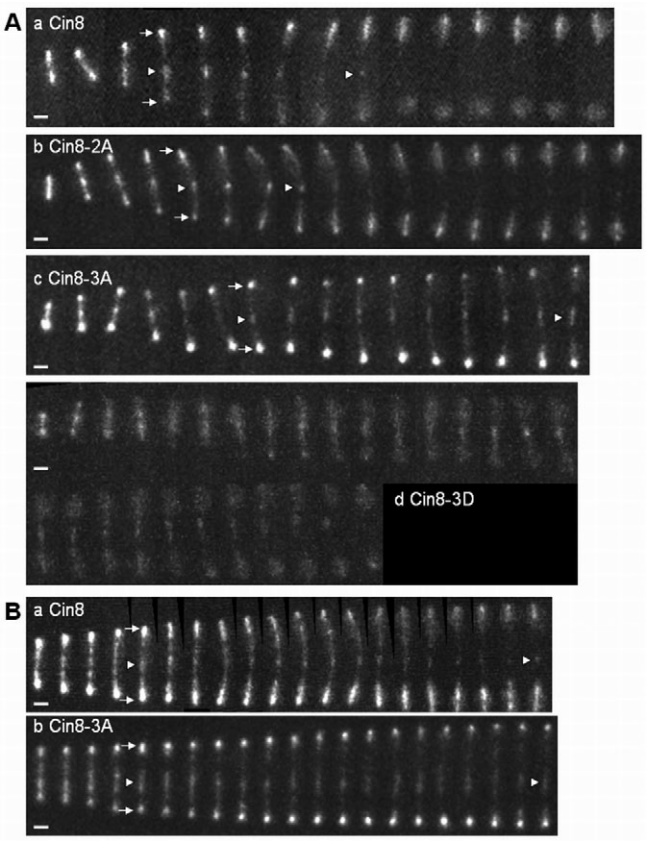

Fig. 2. Anaphase spindle localization of phosphorylation mutants of Cin8–3GFP. (**A**) a, Cin8; b, Cin8-2A, c, Cin8-3A, d, Cin8-3D. Time interval, 1 minute. (**B**) a, Cin8; b, Cin8-3A; time interval, 20 seconds. Scale bar: 1 μm. Arrows indicate spindle poles; arrowheads indicate the midzone.

producing Cin8-3D were not viable at 37°C (supplementary material Fig. S3A). At room temperature, ~65% of the *cin8Δ kip1Δ* cells expressing *cin8-3D* were large-budded with monopolar spindles, compared with only ~10% of the cells expressing *CIN8*. At 37°C, the cells producing Cin8-3D arrested as large-budded cells with collapsed spindles (supplementary material Fig. S3B). These findings indicate that in the absence of Kip1, the reduced binding of Cin8-3D to the spindle interferes with spindle assembly and suggest that dephosphorylation of Cin8 is required to assemble mitotic spindles and maintain their bipolar structures before anaphase.

The phosphorylation-dependent affinity of Cin8 to the spindles might be explained by two mechanisms. The additional negative charge caused by phosphorylation (or mutation to aspartic acid) of residues in the motor domain might directly reduce the affinity of Cin8 for MTs, causing its detachment from the spindle. This is opposed to what has been shown thus far for several kinesin-5 family members, namely that a C-terminal tail domain phosphorylation promotes localization to the mitotic spindle (Blangy et al., 1995; Cahu et al., 2008; Sawin and Mitchison, 1995; Sharp et al., 1999). Here, we show for the first time that phosphorylation of the kinesin-5 Cin8 negatively regulates its localization to the mitotic spindle: its prevention increases Cin8 binding to the spindle. A similar effect of phosphorylation has been shown for the *Caenorhabditis elegans* kinesin-6 homologue ZEN-4: the motor domain phosphorylation by Cdk1 reduced the affinity of ZEN-4 for MTs (Mishima et al., 2004). In addition,

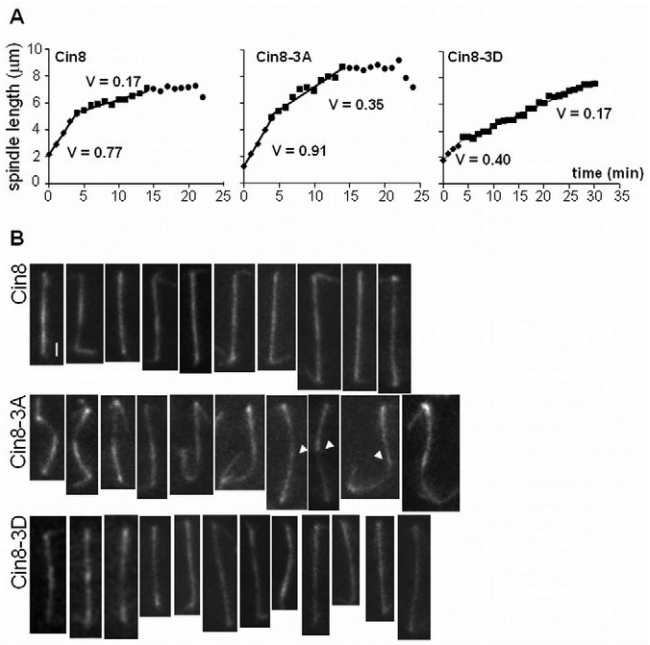

Fig. 3. Anaphase spindle elongation and morphology in cells that express phosphorylation mutants of Cin8. (A) Representative spindle-elongation kinetics in cells producing WT Cin8 (left), Cin8-3A (middle) and Cin8-3D (right). V, rate of spindle elongation (μm/minute). The phases of spindle elongation are indicated as follows: diamonds, fast phase; squares, slow phase; circles, post-anaphase. (B) Long anaphase spindle morphologies in cells expressing tubulin–GFP and Cin8 (top), Cin8-3A (middle) or Cin8-3D (bottom). Scale bar: 1 μm. Arrowheads indicate small overlapping region of the iMTs.

phosphorylation of the conserved serine residue in the motor domain of the *Drosophila melanogaster* kinesin-13, KLP10A, alters the interaction of KLP10A with the MTs and diminishes its MT-depolymerizing activity (Mennella et al., 2009).

An alternative role for Cin8 phosphorylation might be to reduce interactions between Cin8 and accessory spindle binding protein(s). It has recently been shown that Cin8 interacts directly with the conserved MT bundling and midzone-organizing protein Ase1, an interaction that is dependent on Ase1 dephosphorylation (Khmelinskii et al., 2009): delivery of Cin8 to the spindle seems to be controlled by dephosphorylation of Ase1 (Khmelinskii et al., 2009). Our data strongly indicate that spindle detachment of Cin8 is regulated by its own phosphorylation. It is possible that the interaction between Cin8 and Ase1 depends on the phosphorylation state of both proteins, as is the case for the fission yeast kinesin-6 and Ase1 (Fu et al., 2009), and that Cin8 phosphorylation reduces its interaction with Ase1.

Cdk1 phosphorylation of Cin8 regulates its function in mitotic spindle morphogenesis

In *S. cerevisiae* cells, anaphase B consists of two phases, a fast phase followed by a slow one, with Cin8 contributing mainly to the elongation during the fast phase (Straight et al., 1998). To examine the role of phosphorylation in Cin8 function on the spindle, we monitored the anaphase spindle elongation kinetics and the spindle morphology. In Cin8-3D cells (Fig. 2Ad), as well as in *cdc55Δ* cells (supplementary material Fig. S2C), where Cin8 exhibits diminished binding to the spindle compared with WT cells, the spindle elongation rate was considerably slower (Fig. 3A, Table 1 and supplementary material Fig. S2C). However, in Cin8-3A and *clb2Δ* cells, where Cin8 occupies a larger portion of the middle spindle (Fig. 2Ac,Bb and supplementary material Fig. S2B), the spindle elongation rate was considerably faster (Fig. 3A, Table 1 and supplementary material Fig. S2B). Also, in Cin8-3A cells, the overlapping region of antiparallel interpolar MTs (iMTs) is significantly decreased (Fig. 3B, arrowheads and Table 1) and the spindle disassembly is delayed by ~3 minutes (Table 1). Finally, Cin8-3A cells exhibited deformed, bent and asymmetrical spindles (Fig. 3B). Thus our data indicate that phosphorylation of Cin8 controls anaphase spindle elongation.

The higher spindle elongation rate in cells expressing the phosphorylation-deficient Cin8-3A is likely to cause the shorter iMT overlapping region in these cells (Table 1). Because this region serves as a binding site for proteins that control spindle stabilization and iMT plus-end dynamics during anaphase (Buvelot et al., 2003; Fridman et al., 2009; Higuchi and Uhlmann, 2005; Khmelinskii et al., 2007; Schuyler et al., 2003; Thomas and Kaplan, 2007), the decreased size of this region is likely to reduce the stabilization of the iMT plus-ends and thus cause the deformed and asymmetrical spindle morphologies observed in these cells. Hence, our results indicate that the decreased amount of Cin8 at the midzone region at the end of anaphase is required for slowing down the rate of spindle elongation and maintaining the correct structure of the midzone and anaphase spindle.

To summarize, we propose that the phosphorylation–dephosphorylation of Cdk1 sites in Cin8 motor domain controls the binding of a correct amount of Cin8 to the spindle during mitosis. Before the onset of anaphase, Cin8 is dephosphorylated to promote its attachment to the spindle and facilitate its function in spindle assembly. At early–mid anaphase, the activation of Cdc14 phosphatase by the FEAR (Cdc14 early anaphase release) pathway (Chiroli et al., 2009; Ross and Cohen-Fix, 2004; Stegmeier et al., 2002) dephosphorylates Cin8, thus inducing binding of Cin8 to the short anaphase spindle and promoting fast spindle elongation. At late anaphase, when Cdc14 is no longer present at the spindle midzone (Stegmeier et al., 2002) (supplementary material Fig. S4), Cin8 phosphorylation becomes dominant and it detaches from the spindle. This detachment is

Table 1. Effect of Cin8 phosphorylation variants on anaphase spindle elongation

Cin8 variant	Fast-phase rate (μm/minute)	Slow-phase rate (μm/ minute)	Maximal spindle length (μm)	Time before spindle breakage (minutes)	Midzone size (% of spindle length)
WT Cin8	0.82±0.04 (20)	0.22±0.01 (28)	7.72±0.20 (20)	10.24±1.14 (17)	18.9±0.9 (62)
Cin8-3A	0.89±0.03 (43)	0.33±0.02*** (50)	8.31±0.20 (41)	13.83±1.07* (18)	12.9±0.3*** (173)
Cin8-3D	0.41±0.04*** (10)	0.16±0.01** (12)	ND	ND	17.8±1.2 (34)

Values represent mean±s.e.m.; the number of cells analyzed is shown in brackets. *P<0.05; **P<0.01; ***P<0.001, compared with WT cells. The maximal spindle length was determined following spindle disassembly. The time before spindle breakage is the time between the end of slow phase and spindle disassembly. The midzone size was measured for long spindles (>5.5 μm). ND, not determined; few cells were observed in anaphase B.

required for slowing down the rate of spindle elongation to maintain the correct structure of the spindle.

Materials and Methods

Yeast strains

S. cerevisiae strains used are listed in supplementary material Table S1.

Cell growth, cell-cycle arrest and western blot analysis

Cell cycle was arrested after overnight growth to mid-log phase and transfer into the arrest conditions for 3-4 h. The following reagents were applied: for G1 arrest, 5 μg/ml α-factor (Sigma); for S phase, 0.1 M hydroxyurea (Sigma); for metaphase, 10 μg/ml nocodazole (Sigma). To release cells from the S-phase arrest, cells were washed and resuspended in fresh medium lacking hydroxyurea. For late anaphase arrest, cells expressing the *ts* mutations *cdc15-2*, *cdc14-1* or *cdc5-7* were shifted to 37°C. The ability of Cin8 phosphorylation mutants to complement a *CIN8* deletion allele was tested in a strain with deletions in both *CIN8* and *KIP1*. Since *cin8*Δ *kip1*Δ double mutants are not viable, the viability of the tester strain was maintained by a *CIN8* plasmid carrying *CYH2* as well. Despite the presence of a recessive cycloheximide resistance allele *cyh2* in the genome, this strain is sensitive to cycloheximide because of the dominant *CYH2* allele carried on the plasmid (Gheber et al., 1999). At 26°C, transformation with a second plasmid carrying *CIN8*, *cin8-3A* or *cin8-3D*, however, allowed cells to live without the *CIN8-CYH2* plasmid and therefore to grow on cycloheximide-containing medium (supplementary material Fig. S1). Treatment of extracts with CIP phosphatase was previously described (Cohen-Fix and Koshland, 1997). Whole-cell protein extracts were obtained as desribed (Hildebrandt et al., 2006). For 3HA-Cdc14 overexpression during anaphase arrest, *cdc15-2* cells expressing Cin8-13Myc and P_{GAL1}-HA-Cdc14 were grown in 2% raffinose medium to mid-log phase and shifted to 37°C. 2% galactose was added to the medium for 1 or 2 hours, whilst holding the cells at 37°C. The total incubation time at 37°C was 6 hours. For the band-retardation assay, to visualize the slow-migrating band of Cin8 (Fig. 1H), whole-cell extracts were fractionated on a 10% SDS PAGE for 7–9 hours and subjected to western blot analysis. The antibodies used were mouse anti-HA (12CA5, Abcam), mouse anti-Myc (9E10, Santa Cruz) and goat anti-mouse IgG HRP conjugate (W402B, Promega).

In vitro phosphoryalation assay

The TAP method was applied for purification of cyclin Cdc28 complexes from *sic1*ΔP_{GAL}-*CLB2-TAP*, *sic1*ΔP_{GAL}-*CLB3-TAP*, and *sic1*ΔP_{GAL}-*CLB5-TAP* strains, as described previously (Puig et al., 2001; Ubersax et al., 2003). Purification of CIN8-590–TEV–EGFP–6xHIS and Cin8-3A-590–TEV–EGFP–6xHIS was performed using standard cobalt affinity chromatography, and the elution was accomplished with 200 mM imidazole. For the phosphorylation assays of Cin8, about 0.1 mg/ml purified Cin8 was used. The basal composition of the assay mixture contained 50 mM HEPES, pH 7.4, 150 mM NaCl, 80 mM imidazole, 2% glycerol, 2 mM EGTA, 0.25 mg/ml BSA, 80 μg/ml Cks1, and 500 μM ATP [with added [γ-^{32}P]ATP (Perkin Elmer)]. Around 50 nM of the purified kinase complex was used and the reaction was stopped with SDS-PAGE sample buffer.

Imaging and anaphase spindle elongation kinetics

Real-time imaging of GFP-tagged proteins and measurements of the spindle elongation kinetics were previously described (Fridman et al., 2009; Gerson-Gurwitz et al., 2009; Movshovich et al., 2008). In brief, time-lapse *z*-stacks images were acquired with a Zeiss Axiovert 200M-based Nipkow spinning-disc confocal microscope (UltraView ESR, Perkin Elmer, UK) equipped with an EMCCD camera, with 0.2 μm separation between planes and 4–60 second time intervals. Image processing and spindle length measurements (in 3D) were performed using ImageJ and MetaMorph software.

Statistical analysis

The significance of the differences between the average values was determined using Student's *t*-test. **P*<0.05; ***P*<0.01; ****P*<0.001.

DNA manipulation

The N-terminal 6-Myc tag and the C-terminal 3HA tags of Cin8 were previously described (Hildebrandt et al., 2006). A PCR-generated strategy was used to replace *CDC55* open reading frame with SpHIS5 (Delneri et al., 2000) using (f) 5′-TCGATTACGTCAATTAGGCTCTCTTCTATATTTTAGTTCAGATCCGCTAGGGATAACAGG-3′ and (r) 5′-TTTCAATTAAAACAGTAGTAGTATGTGGGGAAGATATGGGTCATCGATGAATTCGAGCTC-3′ primers and the pKT101 plasmid from EUROSCARF collection (Sheff and Thorn, 2004) as a template. The C-terminal 13-Myc tag was constructed using the pKT233 plasmid from EUROSCARF collection (Sheff and Thorn, 2004). The *13Myc* and *ADH1* termination region were PCR-amplified from the pKT233 plasmid using (f) 5′-CGCGAGCGGCCGCCCCGGGTTAATTAACGGTGAAC-3′ and (R) 5′-GAGCGTCTAGACCCTAGCGGATCTGCCGGTAGAG-3′ primers and replacing the *Not*I-*Xba*I fragment of pTK47, creating pRM39. Then, the *Pst*I-*Xba*I fragment was transferred from pRM39 to pTK49 (Hildebrandt et al., 2006), creating pRM40. Finally, the *Sal*I-*Xba*I fragment of *CIN8-13Myc* was transferred to the pRS316 vector, resulting in pJKY1. The C-terminal 3GFP tag of Cin8 was constructed by PCR amplification of the 3GFP sequence using the pB1963 plasmid as a template [a gift from David Pellman's lab (Buttery et al., 2007)] and the (f) 5′-TCAAGCGGCCGCTCCTGCAGCCCGGGGGATCCA-3′ and (r) 5′-ACCGCGGTGGCGGCCGCT-3′ primers. The PCR-amplified sequence was introduced into the C-terminal *Not*I site of *CIN8* (Hildebrandt et al., 2006). For genomic integration of *CIN8-3GFP*, *CIN8-3GFP* was subcloned into the pRS305 vector (Sikorski and Hieter, 1989) and integrated into the *LEU2* locus. Plasmid containing the mutations of the five Cdc28 phosphorylation sites (*cin8-5A*) in pTK49 (Hildebrandt et al., 2006), pYLCIN8 1-5, was a gift from Gavin Sherlock (Cold Spring Harbor Laboratories, Cold Spring Harbor, NY). To construct *6Myc-cin8-5A*, *Aat*II-*Sph*1 fragment of *cin8-5A* sequence was transferred from the pYLCIN8 1-5 plasmid to pTK103 (Hildebrandt et al., 2006). The separation between the Cdc28-kinase phosphorylation sites in the motor domain and the tail of Cin8 was done using the unique *Pst*I site within the *CIN8* sequence. The phosphomimic *cin8-3D* mutations (D277, D285, D493) were generated by PCR site-directed mutagenesis (Ko and Ma, 2005), the following primers were used: (f) 5′-ATGCAAGCTTTGTCGACGTTTTCGCCCCAGGTT-3′, (r) 5′-ATGCGGTCTCAATGACCTAGGGTCACTGTTCCTAGAATTACTCCTGGAACTACTAGC-3′, (f) 5′-ATGCGGTCTCATCATTAAATGATCTGGATCCTAAAGCTGCTCTATTAAGAAAAAGG-3′, (r) 5′-ATGCCTGCAGGTTTCTTCAGAAGTTACCTTTGCAGGATCGATAGTAGCAATTAGTGCGGTTTTCGT-3′. The pRM59 plasmid containing the *3HA-CDC14* coding sequence under the *PGAL1* promoter was constructed by PCR-amplifying the *3HA-CDC14* sequence from the p194 plasmid (a gift from Angelica Amon, MIT Cambridge, MA), using (f) 5′-CGTCGTCTAGACGCTTATAAAAAAAAAAAAAAAATGCG-3′ and (r) 5′-CGGTGAAGTTATTCCTAGGTACCAGG-3′ primers and sub-cloning into the *Kpn*I-*Xba*I sites of p416-GAL1 (Mumberg et al., 1994). For bacteria expression of Cin8 motor domain, first 590 residues of (CIN8-WT) and (cin8-3A) were PCR amplified and cloned into *Nde*I and *Sph*I sites of modified pRSET-B plasmid that contain TEVEGFP–6HIS at the C-terminus, creating pAG26 and pJKY34, respectively. The following primers were used: (f) 5′-AGTCCATATGGTATGGCCAGAAAGTAACGTTGAG-3′, (r) 5′-CTCGAGGCGGCCGCGCGCATGCCTTGCATTTTTCGATGTCAAACTTTCAAT-3′.

We thank David Pellman, Angelica Amon and Gavin Sherlock for providing plasmids and Monica Einav for technical assistance. This work was supported in part by ISF grant no. 1043/09 awarded to L.G. and by a BSF grant 2003141 awarded to L.G. and M.A.H. M.L. was supported by Wellcome Trust International Fellowship 079014/Z/06/Z and a grant from Estonian Science Foundation, ETF 6766. Deposited in PMC for immediate release.

Supplementary material available online at
http://jcs.biologists.org/cgi/content/full/124/6/????/DC1

References

Blangy, A., Lane, H. A., d'Herin, P., Harper, M., Kress, M. and Nigg, E. A. (1995). Phosphorylation by p34cdc2 regulates spindle association of human Eg5, a kinesin-related motor essential for bipolar spindle formation in vivo. *Cell* **83**, 1159-1169.

Buttery, S. M., Yoshida, S. and Pellman, D. (2007). Yeast formins Bni1 and Bnr1 utilize different modes of cortical interaction during the assembly of actin cables. *Mol. Biol. Cell* **18**, 1826-1838.

Buvelot, S., Tatsutani, S. Y., Vermaak, D. and Biggins, S. (2003). The budding yeast Ipl1/Aurora protein kinase regulates mitotic spindle disassembly. *J. Cell Biol.* **160**, 329-339.

Cahu, J., Olichon, A., Hentrich, C., Schek, H., Drinjakovic, J., Zhang, C., Doherty-Kirby, A., Lajoie, G. and Surrey, T. (2008). Phosphorylation by Cdk1 increases the binding of Eg5 to microtubules in vitro and in Xenopus egg extract spindles. *PLoS One* **3**, e3936.

Chee, M. K. and Haase, S. B. (2010). B-cyclin/CDKs regulate mitotic spindle assembly by phosphorylating kinesins-5 in budding yeast. *PLoS Genet.* **6**, e1000935.

Chiroli, E., Rancati, G., Catusi, I., Lucchini, G. and Piatti, S. (2009). Cdc14 inhibition by the spindle assembly checkpoint prevents unscheduled centrosome separation in budding yeast. *Mol. Biol. Cell* **20**, 2626-2637.

Cohen-Fix, O. and Koshland, D. (1997). The anaphase inhibitor of Saccharomyces cerevisiae Pds1p is a target of the DNA damage checkpoint pathway. *Proc. Natl Acad. Sci. USA* **94**, 14361-14366.

Delneri, D., Tomlin, G. C., Wixon, J. L., Hutter, A., Sefton, M., Louis, E. J. and Oliver, S. G. (2000). Exploring redundancy in the yeast genome: an improved strategy for use of the cre-loxP system. *Gene* **252**, 127-135.

Fridman, V., Gerson-Gurwitz, A., Movshovich, N., Kupiec, M. and Gheber, L. (2009). Midzone organization restricts interpolar microtubule plus-end dynamics during spindle elongation. *EMBO Rep.* **10**, 387-393.

Fu, C., Ward, J. J., Loiodice, I., Velve-Casquillas, G., Nedelec, F. J. and Tran, P. T. (2009). Phospho-regulated interaction between kinesin-6 Klp9p and microtubule bundler Ase1p promotes spindle elongation. *Dev. Cell* **17**, 257-267.

Garcia, K., Stumpff, J., Duncan, T. and Su, T. T. (2009). Tyrosines in the kinesin-5 head domain are necessary for phosphorylation by Wee1 and for mitotic spindle integrity. *Curr. Biol.* **19**, 1670-1676.

Gerson-Gurwitz, A., Movshovich, N., Avunie, R., Fridman, V., Moyal, K., Katz, B., Hoyt, M. A. and Gheber, L. (2009). Mid-anaphase arrest in S. cerevisiae cells eliminated for the function of Cin8 and dynein. *Cell. Mol. Life Sci.* **66**, 301-313.

Gheber, L., Kuo, S. C. and Hoyt, M. A. (1999). Motile properties of the kinesin-related Cin8p spindle motor extracted from Saccharomyces cerevisiae cells. *J. Biol. Chem.* **274**, 9564-9572.

Giet, R., Uzbekov, R., Cubizolles, F., Le Guellec, K. and Prigent, C. (1999). The Xenopus laevis aurora-related protein kinase pEg2 associates with and phosphorylates the kinesin-related protein XlEg5. *J. Biol. Chem.* **274**, 15005-15013.

Gordon, D. M. and Roof, D. M. (2001). Degradation of the kinesin Kip1p at anaphase onset is mediated by the anaphase-promoting complex and Cdc20p. *Proc. Natl. Acad. Sci. USA* **98**, 12515-12520.

Goshima, G. and Vale, R. D. (2005). Cell cycle-dependent dynamics and regulation of mitotic kinesins in Drosophila S2 cells. *Mol. Biol. Cell* **16**, 3896-3907.

Grandin, N. and Reed, S. I. (1993). Differential function and expression of Saccharomyces cerevisiae B-type cyclins in mitosis and meiosis. *Mol. Cell. Biol.* **13**, 2113-2125.

Hagan, I. and Yanagida, M. (1992). Kinesin-related cut7 protein associates with mitotic and meiotic spindles in fission yeast. *Nature* **356**, 74-76.

Heck, M. M., Pereira, A., Pesavento, P., Yannoni, Y., Spradling, A. C. and Goldstein, L. S. (1993). The kinesin-like protein KLP61F is essential for mitosis in Drosophila. *J. Cell Biol.* **123**, 665-679.

Higuchi, T. and Uhlmann, F. (2005). Stabilization of microtubule dynamics at anaphase onset promotes chromosome segregation. *Nature* **433**, 171-176.

Hildebrandt, E. R. and Hoyt, M. A. (2001). Cell cycle-dependent degradation of the Saccharomyces cerevisiae spindle motor Cin8p requires APC(Cdh1) and a bipartite destruction sequence. *Mol. Biol. Cell* **12**, 3402-3416.

Hildebrandt, E. R., Gheber, L., Kingsbury, T. and Hoyt, M. A. (2006). Homotetrameric form of Cin8p, a Saccharomyces cerevisiae kinesin-5 motor, is essential for its in vivo function. *J. Biol. Chem.* **281**, 26004-26013.

Hoyt, M. A., He, L., Loo, K. K. and Saunders, W. S. (1992). Two Saccharomyces cerevisiae kinesin-related gene products required for mitotic spindle assembly. *J. Cell Biol.* **118**, 109-120.

Jaspersen, S. L., Charles, J. F., Tinker-Kulberg, R. L. and Morgan, D. O. (1998). A late mitotic regulatory network controlling cyclin destruction in Saccharomyces cerevisiae. *Mol. Biol. Cell* **9**, 2803-2817.

Kapitein, L. C., Peterman, E. J., Kwok, B. H., Kim, J. H., Kapoor, T. M. and Schmidt, C. F. (2005). The bipolar mitotic kinesin Eg5 moves on both microtubules that it crosslinks. *Nature* **435**, 114-118.

Kashina, A. S., Rogers, G. C. and Scholey, J. M. (1997). The bimC family of kinesins: essential bipolar mitotic motors driving centrosome separation. *Biochim. Biophys. Acta* **1357**, 257-271.

Khmelinskii, A., Lawrence, C., Roostalu, J. and Schiebel, E. (2007). Cdc14-regulated midzone assembly controls anaphase B. *J. Cell Biol.* **177**, 981-993.

Khmelinskii, A., Roostalu, J., Roque, H., Antony, C. and Schiebel, E. (2009). Phosphorylation-dependent protein interactions at the spindle midzone mediate cell cycle regulation of spindle elongation. *Dev. Cell* **17**, 244-256.

Ko, J. K. and Ma, J. (2005). A rapid and efficient PCR-based mutagenesis method applicable to cell physiology study. *Am. J. Physiol. Cell Physiol.* **288**, C1273-C1278.

Kull, F. J., Sablin, E. P., Lau, R., Fletterick, R. J. and Vale, R. D. (1996). Crystal structure of the kinesin motor domain reveals a structural similarity to myosin. *Nature* **380**, 550-555.

Langan, T. A., Gautier, J., Lohka, M., Hollingsworth, R., Moreno, S., Nurse, P., Maller, J. and Sclafani, R. A. (1989). Mammalian growth-associated H1 histone kinase: a homolog of cdc2+/CDC28 protein kinases controlling mitotic entry in yeast and frog cells. *Mol. Cell. Biol.* **9**, 3860-3868.

Mennella, V., Tan, D. Y., Buster, D. W., Asenjo, A. B., Rath, U., Ma, A., Sosa, H. J. and Sharp, D. J. (2009). Motor domain phosphorylation and regulation of the Drosophila kinesin 13, KLP10A. *J. Cell Biol.* **186**, 481-490.

Mishima, M., Pavicic, V., Gruneberg, U., Nigg, E. A. and Glotzer, M. (2004). Cell cycle regulation of central spindle assembly. *Nature* **430**, 908-913.

Movshovich, N., Fridman, V., Gerson-Gurwitz, A., Shumacher, I., Gertsberg, I., Fich, A., Hoyt, M. A., Katz, B. and Gheber, L. (2008). Slk19-dependent mid-anaphase pause in kinesin-5-mutated cells. *J. Cell Sci.* **121**, 2529-2539.

Mumberg, D., Muller, R. and Funk, M. (1994). Regulatable promoters of Saccharomyces cerevisiae: comparison of transcriptional activity and their use for heterologous expression. *Nucl. Acids Res.* **22**, 5767-5768.

Park, C. J., Song, S., Lee, P. R., Shou, W., Deshaies, R. J. and Lee, K. S. (2003). Loss of CDC5 function in Saccharomyces cerevisiae leads to defects in Swe1p regulation and Bfa1p/Bub2p-independent cytokinesis. *Genetics* **163**, 21-33.

Puig, O., Caspary, F., Rigaut, G., Rutz, B., Bouveret, E., Bragado-Nilsson, E., Wilm, M. and Seraphin, B. (2001). The tandem affinity purification (TAP) method: a general procedure of protein complex purification. *Methods* **24**, 218-229.

Queralt, E., Lehane, C., Novak, B. and Uhlmann, F. (2006). Downregulation of PP2A(Cdc55) phosphatase by separase initiates mitotic exit in budding yeast. *Cell* **125**, 719-732.

Ross, K. E. and Cohen-Fix, O. (2004). A role for the FEAR pathway in nuclear positioning during anaphase. *Dev. Cell* **6**, 729-735.

Sablin, E. P., Kull, F. J., Cooke, R., Vale, R. D. and Fletterick, R. J. (1996). Crystal structure of the motor domain of the kinesin-related motor ncd. *Nature* **380**, 555-559.

Saunders, W. S., Koshland, D., Eshel, D., Gibbons, I. R. and Hoyt, M. A. (1995). Saccharomyces cerevisiae kinesin- and dynein-related proteins required for anaphase chromosome segregation. *J. Cell Biol.* **128**, 617-624.

Sawin, K. E. and Mitchison, T. J. (1995). Mutations in the kinesin-like protein Eg5 disrupting localization to the mitotic spindle. *Proc. Natl. Acad. Sci. USA* **92**, 4289-4293.

Schuyler, S. C., Liu, J. Y. and Pellman, D. (2003). The molecular function of Ase1p: evidence for a MAP-dependent midzone-specific spindle matrix. Microtubule-associated proteins. *J. Cell Biol.* **160**, 517-528.

Sharp, D. J., McDonald, K. L., Brown, H. M., Matthies, H. J., Walczak, C., Vale, R. D., Mitchison, T. J. and Scholey, J. M. (1999). The bipolar kinesin, KLP61F, cross-links microtubules within interpolar microtubule bundles of Drosophila embryonic mitotic spindles. *J. Cell Biol.* **144**, 125-138.

Sheff, M. A. and Thorn, K. S. (2004). Optimized cassettes for fluorescent protein tagging in Saccharomyces cerevisiae. *Yeast* **21**, 661-670.

Shenoy, S., Choi, J. K., Bagrodia, S., Copeland, T. D., Maller, J. L. and Shalloway, D. (1989). Purified maturation promoting factor phosphorylates pp60c-src at the sites phosphorylated during fibroblast mitosis. *Cell* **57**, 763-774.

Sikorski, R. S. and Hieter, P. (1989). A system of shuttle vectors and yeast host strains designed for efficient manipulation of DNA in Saccharomyces cerevisiae. *Genetics* **122**, 19-27.

Spellman, P. T., Sherlock, G., Zhang, M. Q., Iyer, V. R., Anders, K., Eisen, M. B., Brown, P. O., Botstein, D. and Futcher, B. (1998). Comprehensive identification of cell cycle-regulated genes of the yeast Saccharomyces cerevisiae by microarray hybridization. *Mol. Biol. Cell* **9**, 3273-3297.

Stegmeier, F., Visintin, R. and Amon, A. (2002). Separase, polo kinase, the kinetochore protein Slk19, and Spo12 function in a network that controls Cdc14 localization during early anaphase. *Cell* **108**, 207-220.

Straight, A. F., Sedat, J. W. and Murray, A. W. (1998). Time-lapse microscopy reveals unique roles for kinesins during anaphase in budding yeast. *J. Cell Biol.* **143**, 687-694.

Thomas, S. and Kaplan, K. B. (2007). A Bir1p-Sli15p kinetochore passenger complex regulates septin organization during anaphase. *Mol. Biol. Cell* **25**, 25.

Touitou, I., Lhomond, G. and Pruliere, G. (2001). Boursin, a sea urchin bimC kinesin protein, plays a role in anaphase and cytokinesis. *J. Cell Sci.* **114**, 481-491.

Ubersax, J. A., Woodbury, E. L., Quang, P. N., Paraz, M., Blethrow, J. D., Shah, K., Shokat, K. M. and Morgan, D. O. (2003). Targets of the cyclin-dependent kinase Cdk1. *Nature* **425**, 859-864.

Woehlke, G., Ruby, A. K., Hart, C. L., Ly, B., Hom-Booher, N. and Vale, R. D. (1997). Microtubule interaction site of the kinesin motor. *Cell* **90**, 207-216.

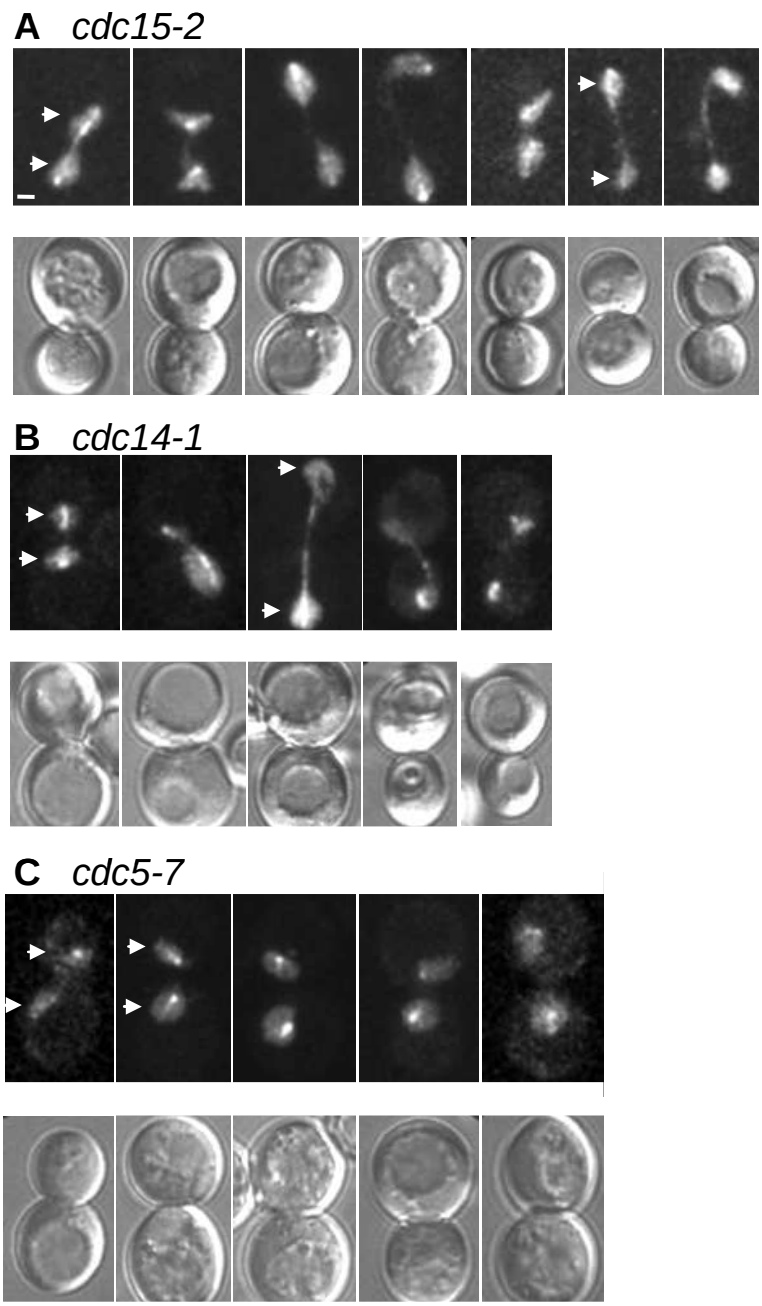

Localization of Cin8-GFP in (A) *cdc15-2*, (B) *cdc14-1* and (C) *cdc5-7* cells arrested in anaphase at 37^{o}C for 2 h. Representative 2D projections are shown. Upper panels – Cin8-GFP, lower panels – corresponding bright field images. Bar, 1 μm. In all cells arrested at late anaphase, a large portion of Cin8-GFP is localized diffusively in the divided nuclei (arrows). Strains are: LGY2968, LGY2974 and LGY2986.

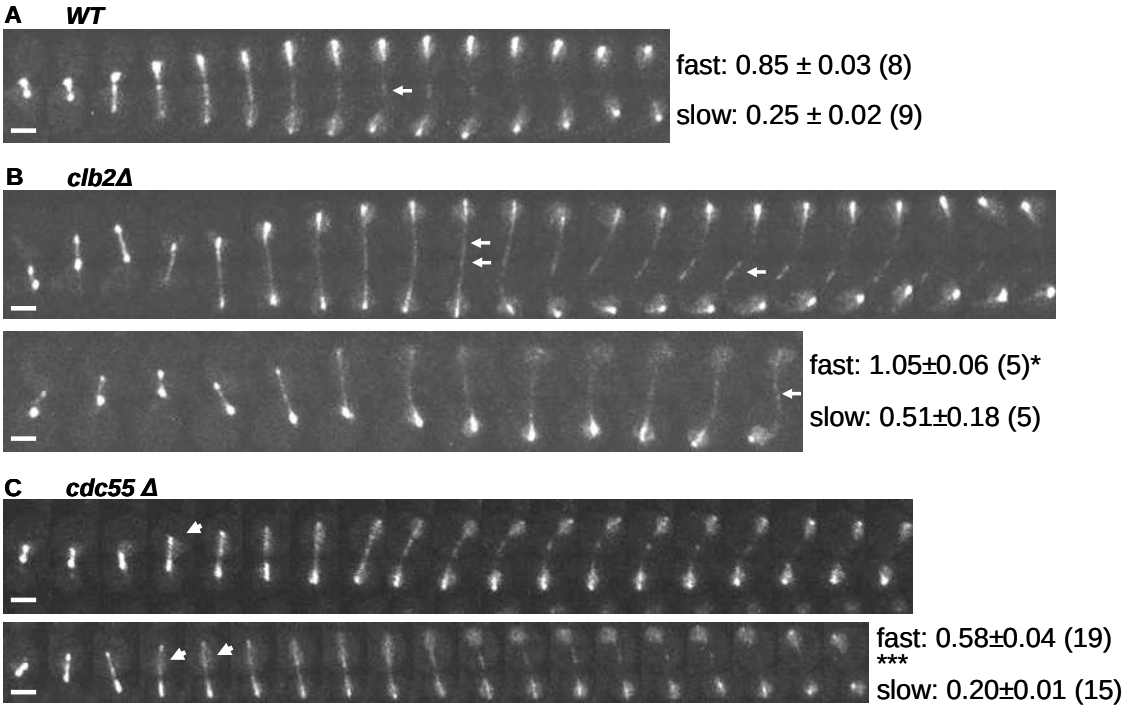

Localization of Cin8-3GFP in (A) WT, (B) *clb2Δ* and (C) *cdc55*Δ cells. 2D projection images of time lapse recording are shown. In B and C, two representative cells in each genotype are shown. Time interval between frames, 2 min. Bar, 2 μm. Strains are: LGY 2533, LGY3033 and LGY 3021. In A and B, arrows indicate Cin8 localization to the middle region of the spindle. In C, small arrows indicate diffusive localization of Cin8 in early-mid anaphase, which is not present in WT cells. Spindle elongation rates (μm/min, average ± SEM) during the fast and the slow phases for each genotype are indicated. The number of measurements is indicated in parentheses.

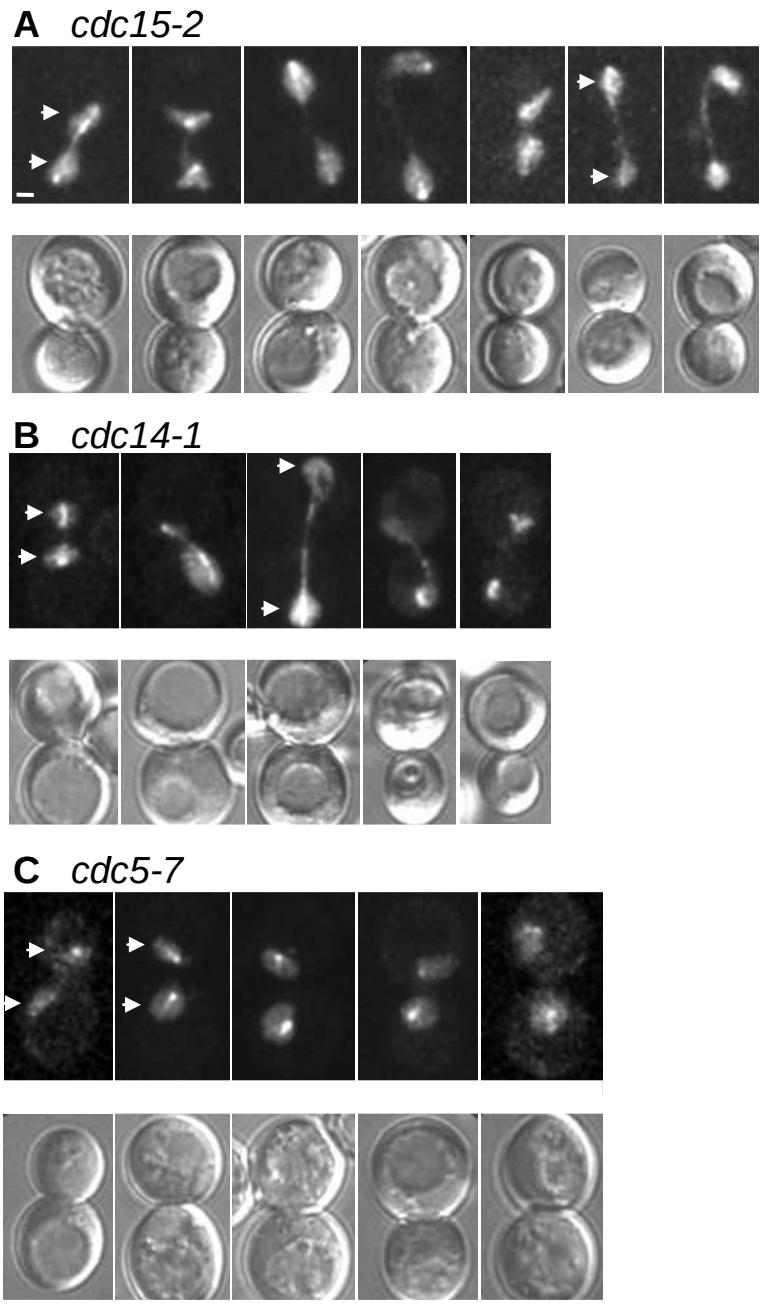

Localization of Cin8-GFP in (A) *cdc15-2*, (B) *cdc14-1* and (C) *cdc5-7* cells arrested in anaphase at 37^{o}C for 2 h. Representative 2D projections are shown. Upper panels – Cin8-GFP, lower panels – corresponding bright field images. Bar, 1 μm. In all cells arrested at late anaphase, a large portion of Cin8-GFP is localized diffusively in the divided nuclei (arrows). Strains are: LGY2968, LGY2974 and LGY2986.

Figure S2

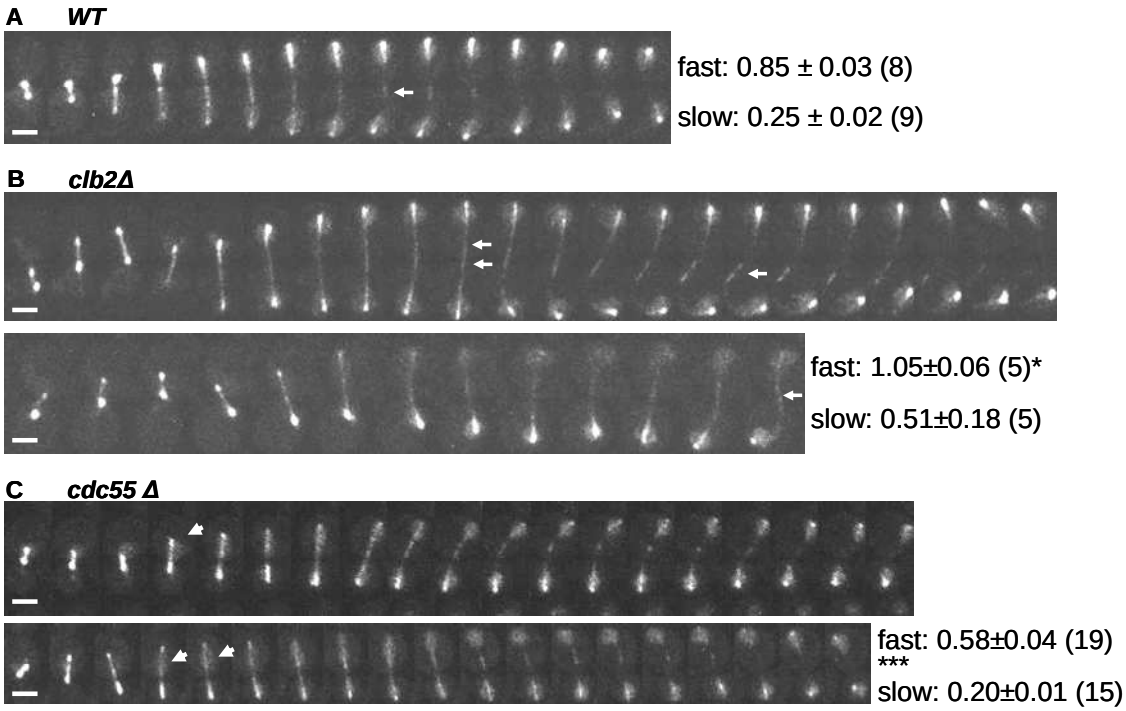

Localization of Cin8-3GFP in (A) WT, (B) *clb2Δ* and (C) *cdc55*Δ cells. 2D projection images of time lapse recording are shown. In B and C, two representative cells in each genotype are shown. Time interval between frames, 2 min. Bar, 2 μm. Strains are: LGY 2533, LGY3033 and LGY 3021. In A and B, arrows indicate Cin8 localization to the middle region of the spindle. In C, small arrows indicate diffusive localization of Cin8 in early-mid anaphase, which is not present in WT cells. Spindle elongation rates (μm/min, average ± SEM) during the fast and the slow phases for each genotype are indicated. The number of measurements is indicated in parentheses.

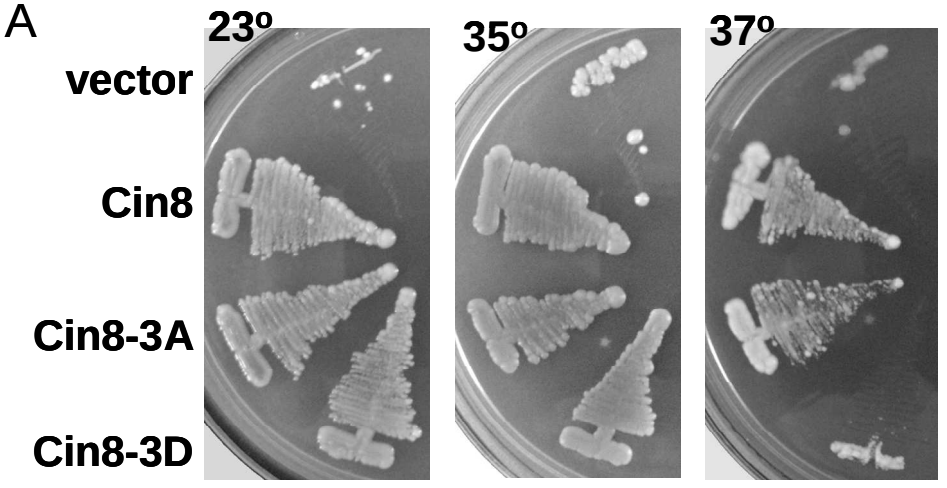

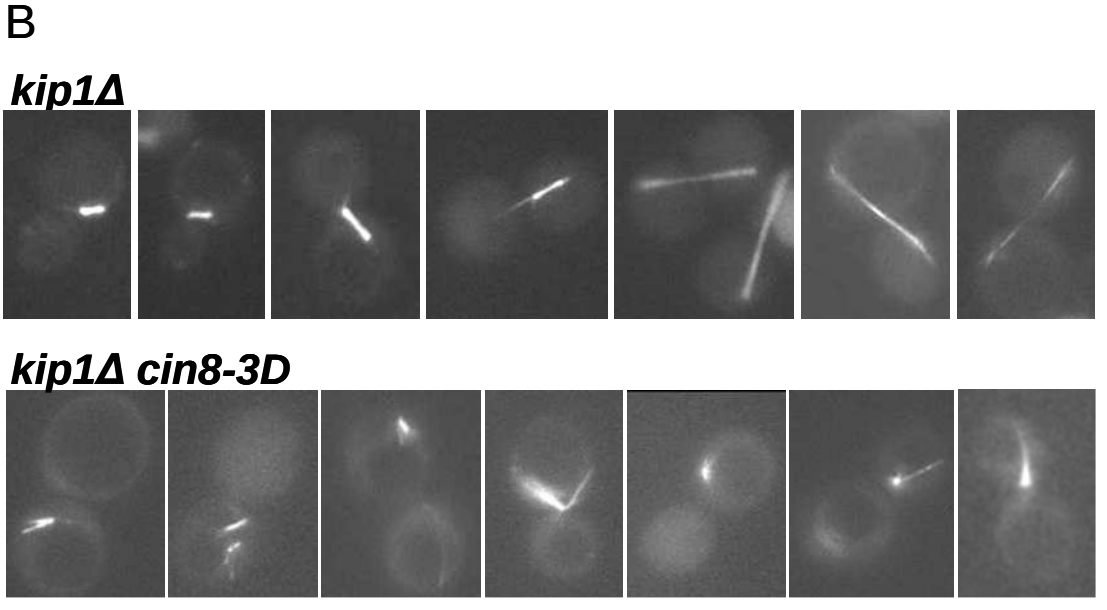

A. Viability of *cin8Δkip1Δ* cells expressing phosphorylation mutants of Cin8 from a CEN plasmid at various temperatures (indicated on top of each panel) on YPD plates containing 5 μg/ml cyclohexamide. Stains are: (LGY2038, LGY2544, LGY2547, LGY2554). **B.** Spindle morphologies of cells *cin8Δkip1Δ* expressing either Cin8 (LGY2544, top panel) or Cin8-3D (LGY2554, bottom panel), grown for 4 h at 37^{o}C. Bar; 2 μm.

Figure S4

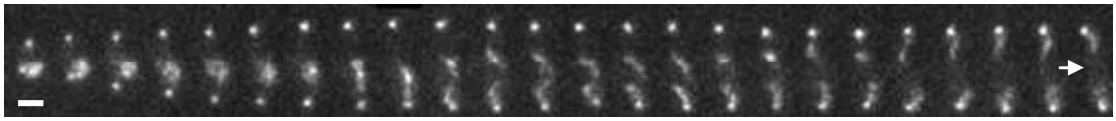

Anaphase spindle localization of Cdc14-GFP in *kip1*Δ cells expressing Nuf2-GFP. Bar, 2 μm; Time intervals, 1 min. For details see (Movshovich et al., 2008). At late anaphase, Cdc14-GFP is not localized to the midzone region (arrow).

Supplementary Figures

Figure S1

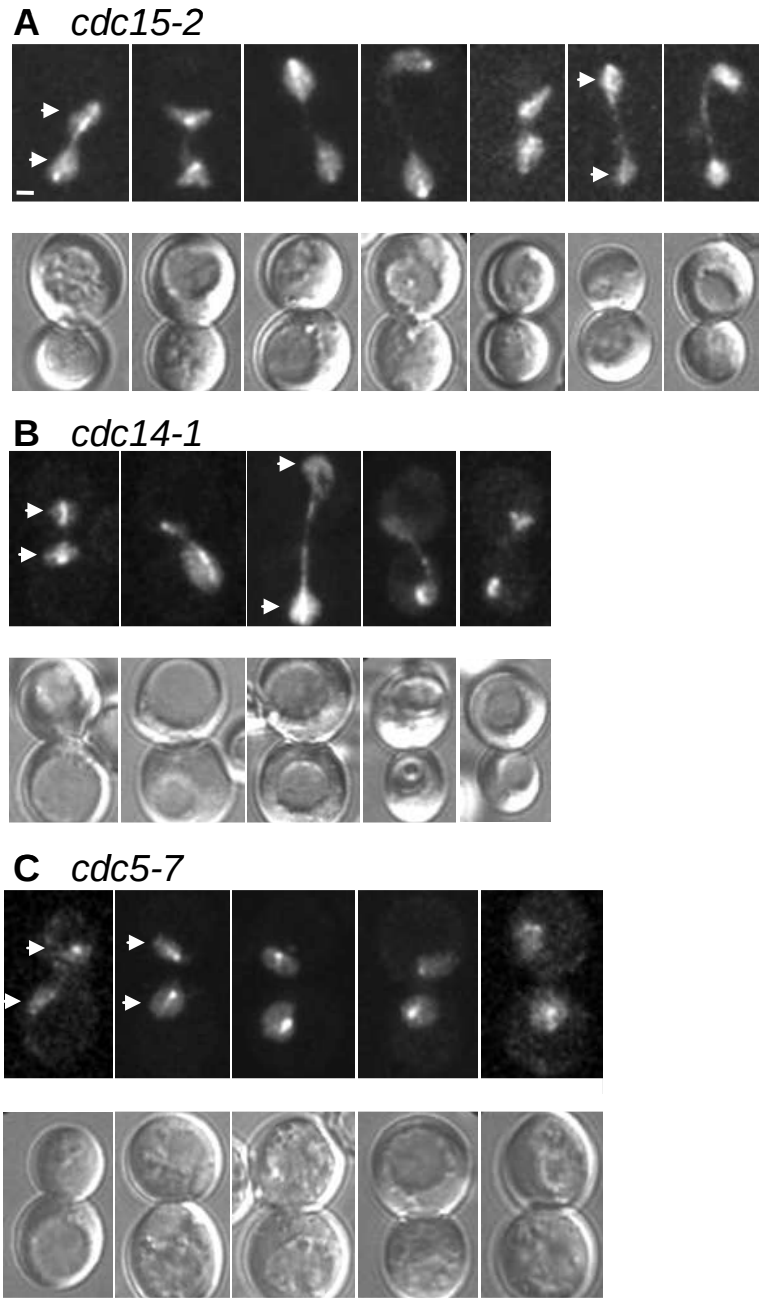

Localization of Cin8-GFP in (A) *cdc15-2*, (B) *cdc14-1* and (C) *cdc5-7* cells arrested in anaphase at 37^{o}C for 2 h. Representative 2D projections are shown. Upper panels – Cin8-GFP, lower panels – corresponding bright field images. Bar, 1 μm. In all cells arrested at late anaphase, a large portion of Cin8-GFP is localized diffusively in the divided nuclei (arrows). Strains are: LGY2968, LGY2974 and LGY2986.

Figure S2

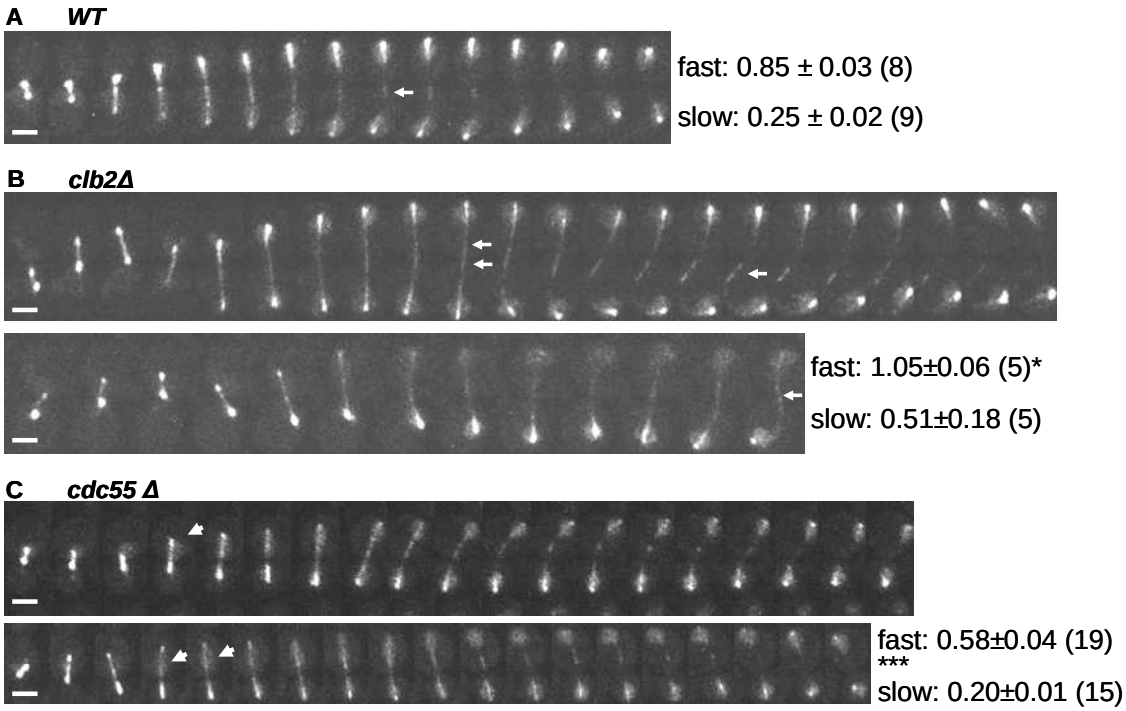

Localization of Cin8-3GFP in (A) WT, (B) *clb2Δ* and (C) *cdc55*Δ cells. 2D projection images of time lapse recording are shown. In B and C, two representative cells in each genotype are shown. Time interval between frames, 2 min. Bar, 2 μm. Strains are: LGY 2533, LGY3033 and LGY 3021. In A and B, arrows indicate Cin8 localization to the middle region of the spindle. In C, small arrows indicate diffusive localization of Cin8 in early-mid anaphase, which is not present in WT cells. Spindle elongation rates (μm/min, average ± SEM) during the fast and the slow phases for each genotype are indicated. The number of measurements is indicated in parentheses.

Figure S3

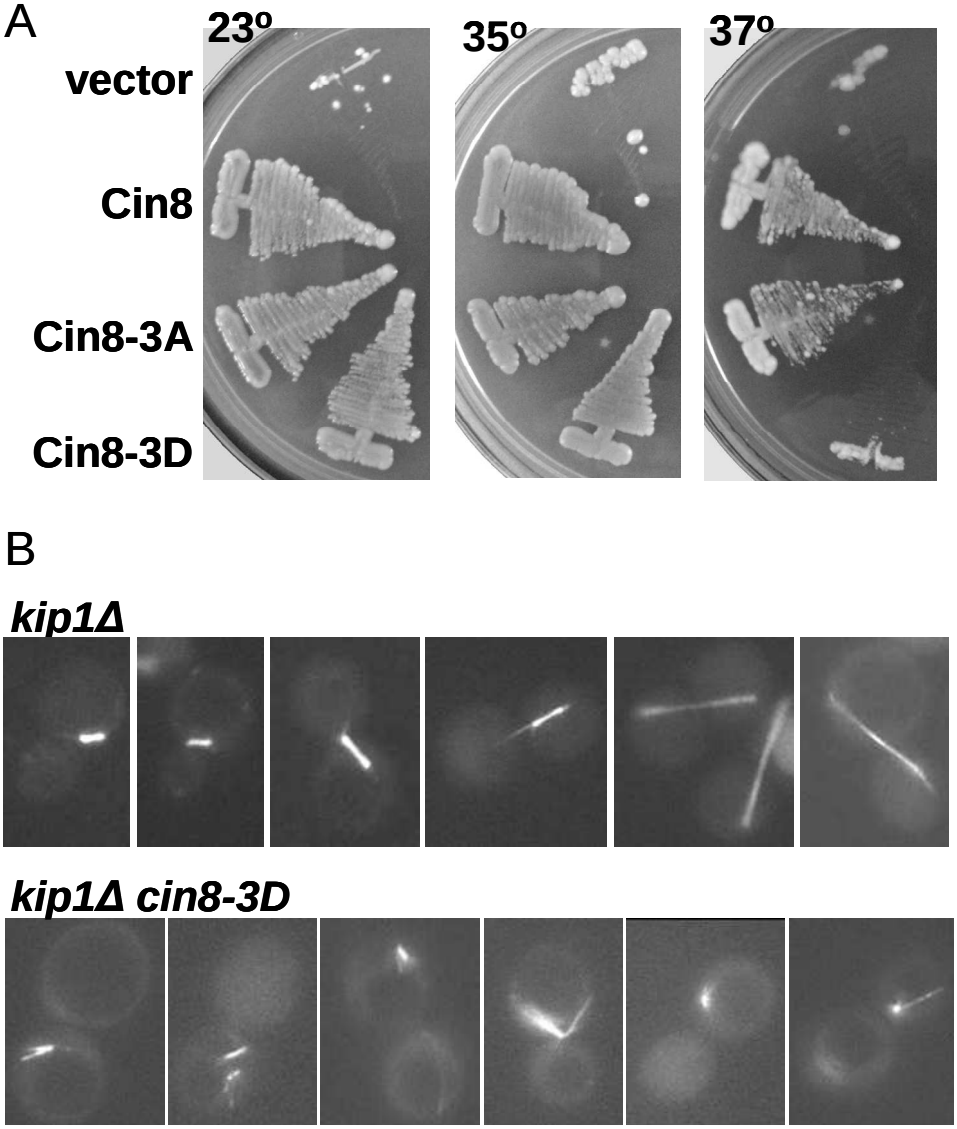

A. Viability of *cin8Δkip1Δ* cells expressing phosphorylation mutants of Cin8 from a CEN plasmid at various temperatures (indicated on top of each panel) on YPD plates containing 5 μg/ml cyclohexamide. Stains are: (LGY2038, LGY2544, LGY2547, LGY2554). **B.** Spindle morphologies of cells *cin8Δkip1Δ* expressing either Cin8 (LGY2544, top panel) or Cin8-3D (LGY2554, bottom panel), grown for 4 h at 37^{o}C. Bar; 2 μm.

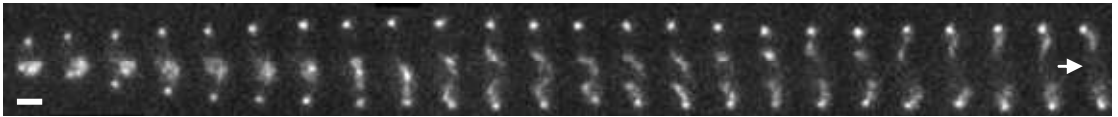

Anaphase spindle localization of Cdc14-GFP in *kip1*Δ cells expressing Nuf2-GFP. Bar, 2 μm; Time intervals, 1 min. For details see (Movshovich et al., 2008). At late anaphase, Cdc14-GFP is not localized to the midzone region (arrow).

Supplementary Table S1

S. cerevisiae strains (S288C) and plasmids used in this study

Strain #	Genotype
LGY 369	*MATa, ura3, leu2, his3, lys2, ade2, cin8Δ::HIS3, cyh2^r,kip1Δ::HIS3*, pTK138
LGY 370	*MATa, ura3, leu2, his3, lys2, ade2, cin8Δ::HIS3, cyh2^r, kip1Δ::HIS3*, pFC23
LGY 1088 (W303)	*MATa, his3, leu2, cdc5::KanMX6, TRP1::cdc5-7*, pTK138
LGY 1092	*MATa, ura3, leu2, his3, ade2, cdc14-1*, pTK138
LGY 1320	*MATa, ura3, leu2, his3, lys2, cdc15-2*, pTK103
LGY 1610	*MATa, ura3, leu2, his3, lys2, cdc15-2*, pRM27
LGY 1715	*MATa, ura3, leu2, his3, lys2, cdc15-2*, pRM28
LGY 1717	*MATa, ura3, leu2, his3, lys2, cdc15-2*, pRM29
LGY 1765	*MATa, ura3, leu2, his3, ade2, GAL+*, pRM18
LGY 1769	*MATa, ura3, leu2, his3, ade2, GAL+, spo12Δ::KanMX6*, pRM18
LGY 2038	*MATa, ura3, leu2, his3, lys2, ade2, cyh2^r, cin8Δ::HIS3, kip1Δ::HIS3*, pMA1208, pRS316
LGY 2055	*MATa, ura3, leu2, his3, lys2, ade2, cin8Δ::URA3, leu2::CIN8-3GFP-LEU2*
LGY 2058	*MATa, ura3, leu2, his3, lys2, ade2, cin8Δ::URA3, leu2::cin8-3A-3GFP-LEU2*
LGY 2237	*MATa, ura3, leu2, lys2, ade2, cin8Δ::URA3, leu2::cin8-3A-3HA-LEU2, his3::TUB1-GFP-HIS3*
LGY 2360	*MATa, ura3, leu2, his3, ade2, GAL+*, pJKY1
LGY 2366	*MATa, ura3, leu2, his3, lys2, cdc15-2*, pJKY1
LGY 2374	*MATa, ura3, leu2, his3, lys2, ade2, cin8Δ::URA3, leu2::CIN8-3HA-LEU2, his3::TUB1-GFP-HIS3*
LGY 2424	*MATa, ura3, leu2, his3, ade2, GAL+, cdc55Δ::SpHIS5*, pJKY1
LGY 2426	*MATa, ura3, leu2, his3, ade2, GAL+, cdc55Δ::SpHIS5*, pJKY2
LGY 2467	*MATa, ura3, leu2, his3, lys2, cdc15-2*, pRM59, pRM40
LGY 2533	*MATa, ura3, leu2, his3, ade2*, GAL+, pVF37
LGY 2544	*MATa, ura3, leu2, his3, lys2, ade2, cyh2^r, cin8Δ::HIS3, kip1::HIS3*, pJKY1
LGY 2547	*MATa, ura3, leu2, his3, lys2, ade2, cyh2^r, cin8Δ::HIS3, kip1::HIS3*, pJKY2
LGY 2554	*MATa, ura3, leu2, his3, lys2, ade2, cyh2^r, cin8Δ::HIS3, kip1::HIS3*, pJKY12
LGY 2685	*MATa, ura3, leu2, his3, lys2, ade2, cin8Δ::URA3, leu2::cin8-2A-3GFP-LEU2*
LGY 2575	*MATa, ura3, leu2, his3, lys2,cin8Δ::URA3, leu2::cin8-3D-3GFP-LEU2*

LGY 2716	*MATa, ura3, leu2, his3, lys2, ade2, cin8Δ::URA3, leu2::cin8-3D-3HA-LEU2, his3::TUB1-GFP-HIS3*
LGY2968	*MATα, ura3, leu2, his3, lys2, cdc15-2,* pVF23
LGY2974	*MATα, ura3, leu2, his3, ade2, cdc14-1,* pVF23
LGY2986 (W303)	*MATa, his3, leu2, cdc5::KanMX6, TRP1::cdc5-7,* pVF23
LGY3001	*MATa, ura3, leu2, his3, ade2, GAL+, cdc55Δ::SpHIS5, leu2::TUB1-GFP-HIS3*
LGY3021	*MATa, , ura3, leu2, his3, ade2,* GAL+, *cdc55Δ::SpHIS5,* pVF37
LGY3033	*MATα, his3Δ1, leu2Δ0, lys2Δ0, ura3Δ0, clb2Δ::KanMX6,* pVF37
Plasmids	
pFC23	*CIN8, LEU, 2μ*
pJKY1	*CIN8-13myc,URA3, CEN* (this study)
pJKY2	*cin8-3A-13myc, URA3, CEN* (this study)
pJKY12	*cin8-3D-13myc, URA3, CEN* (this study)
pRM18	6myc-*CIN8, URA3, CEN* (this study)
pRM27	6myc-*cin8-5A, LYS, CEN* (this study)
pRM28	6myc-*cin8-3A, LYS, CEN* (this study)
pRM29	6myc-*cin8-2A, LYS, CEN* (this study)
pRM39	C-terminus of *CIN8-13myc* in pTZ18 (this study)
pRM40	*CIN8-13myc, LYS, CEN* (this study)
pRM59	P_{GAL1}*-3HA-CDC14, URA, CEN* (this study)
pTK47	*Pst*I-*Xba*I fragment of *CIN8* tail containing *Not*I site before the stop codon in pTZ18, (Kingsbury and Hoyt, unpublished)
pTK103	*6myc-CIN8, LYS2, CEN*
pTK138	*6myc-CIN8, LEU, 2μ*
pMA1208	*CIN8, CYH2, LEU2, CEN*
pRS316	*URA3, CEN*
pAG26	*CIN8-590-TEV-EGFP-6HIS* (pRSET B, bacterial expression, this study)
pJKY34	*cin8-3A-590-TEV-EGFP-6HIS* (pRSET B, bacterial expression, this study)
pVF23	p*CIN8-TEV-GFP-6HIS, URA, CEN* (this study)
pVF37	p*CIN8-3GFP, URA, CEN* (this study)